Voltammetric determination of aluminium(III) at tannic acid capped-gold nanoparticle complexes

Alex L. Suherman[1], Eden E. L. Tanner[1,†], Sabine Kuss[1], Stanislav V. Sokolov[1], Jennifer Holter[2], Neil P. Young[2], Richard G. Compton[1,*]

[1] Department of Chemistry, Physical and Theoretical Chemistry Laboratory, University of Oxford, South Parks Road, Oxford OX1 3QZ, United Kingdom

[2] Department of Materials, University of Oxford, Parks Road, OX1 3PH, UK

*Corresponding author:

[†] Now at the School of Engineering & Applied Sciences, Harvard University, Cambridge, MA, USA.

Emails : richard.compton@chem.ox.ac.uk

Phone : +44 (0) 1865 275957

Fax : +44 (0) 1865 275410

Abstract

The contamination of drinking water and food products by aluminium represents a serious health issue, as it is associated with chronic neurodegenerative diseases. Herein we report an analytical electrochemical method for the determination of aluminium(III) at glassy carbon electrodes, modified with commercially available tannic acid-capped gold nanoparticles. The combination of gold nanoparticles and tannic acid as capping/chelating agent results in an accurate and sensitive detection of aluminium(III) in aqueous solutions by square wave voltammetry (SWV). Employing the presented methodology, clear measurable signals are seen even at the low limit of 10.0 pM, markedly and usefully lower than the permissible level of 7.4 μM for drinking water as defined by the WHO and which compares favourably with alternative detection methods.

Keywords: aluminium(III), tannic acid, gold nanoparticles, metal-complex, square wave voltammetry

1. Introduction

The contamination of drinking water and food products by aluminium represents a serious health issue[1], as it has been associated with the occurrence of Alzheimer's disease[2], Parkinson's dementia[3], renal osteodystrophy[4], and chronic kidney disease[5]. The World Health Organization (WHO) has reported acceptable levels for aluminium of ≤3.7 μM and ≤7.4 μM in treated water for large and small water treatment facilities, respectively.[6] Thus, a highly sensitive detection method that is reliable and simple for the routine monitoring of aluminium(III) in drinking water and food products is needed.

The analytical determination of aluminium(III) has conventionally been performed using atomic absorption spectrometry (AAS)[7], inductively coupled plasma atomic emission spectrometry (ICP-AES)[8], inductively coupled plasma-mass spectrometry (ICP-MS)[9], neutron activation analysis (NAA)[10], electrothermal atomic absorption spectrometry (ETAAS)[11], UV-vis diffuse reflectance spectroscopy (UV-vis DRS)[12] and spectrophotometry[13]. Although these methods offer reasonable sensitivity and reliability, drawbacks, such as extensive sample preparation, required expertise in handling, expensive instrumentation, and the limitation to ex situ analysis, cannot be avoided. Voltammetry with its high sensitivity, rapid analysis time, cost efficiency, and possible adaptation for in situ analysis is an ideal technique for the routine monitoring of sample contamination by aluminium(III). In the literature, the determination of aluminium(III) in aqueous solution by voltammetry was achieved via metal-complexation in the presence of complexing agents, such as 1,2-dihydroxyanthraquinone-3-sulfonic acid (DASA)[14], alizarin S[15], alizarin violet[16], pyrogallol red[17], 8-hydroxyquinoline[18], cupferron[19], and ionophore JS-1[20]; using thin mercury film electrodes (TMFE), renewable silver amalgam film electrodes (Hg(Ag)Fe), multi-walled carbon nanotube modified carbon paste electrodes (MWCNT/CPE), mercury electrodes, hanging mercury dropping electrodes (HMDE), HMDEs, and screen-printed carbon electrodes, respectively. Although these chelating agents have shown the capability to form a metal-complex with aluminium ions (Al^{3+}), it is desirable to use alternative materials with a stronger and more selective binding with Al^{3+}.

Herein, we report the electrochemical determination of Al^{3+} in aqueous solutions at a tannic acid-capped gold nanoparticle modified glassy carbon macroelectrode (**Scheme 1**) using cyclic and square wave voltammetry. Because of their high activity towards many chemical reactions, including molecular adsorption[21], reduction process[22], and metal complexes[23, 24], metallic nanoparticles are extensively studied in areas of catalysis, sensing, and electronic applications. In the present work, the large surface area to mass ratio of nanoparticles is exploited alongside their use to support chemically selective capping agents. Specifically, by drop casting nanoparticles, the surface area of an electrode is much increased and permits an enhanced analytical performance, resulting in lower levels of detection during sensing applications. Moreover, since the aggregation/agglomeration of gold nanoparticles ideally needs to be avoided[25-27], employing gold nanoparticles (AuNPs) in combination with tannic acid ($C_{76}H_{52}O_{46}$, TA) as a capping agent, has been shown to minimise this effect.[28, 29]

In plants, TA is a naturally occurring polymer, exhibiting a range of structures, molecular masses, and physicochemical and biological properties[30, 31]. TA consists of a central glucose core

and surrounding covalently attached digalloyl ester groups, containing reactive functional groups, such as hydroxyl and phenolic hydroxyl, which can bind metals[31, 32]. Generally, the catechol or galloyl groups of TA provide binding sites for metal ions, ranging from mono-type to tris-type complexes[30, 33]. Diverse metals and heavy metal ions such as Fe(III)[32], Ti(IV)[34], Hg(II)[35], Pb(II)[36], Cu(II)[37], Ni(II)[38], and Al(III)[39, 40] are reported to complex with TA by adsorption. Stability constants of these complexes, indicating the affinity of the metal with TA, differ, and much higher values have been reported in the literature for Al^{3+} than for other ions[30, 34, 40-43]. This suggests the use of TA for the selective detection of Al^{3+}. The proposed methodology below is based on the complexation process between Al^{3+} and TA, at tannic acid capped-gold nanoparticles, drop casted onto a modified glassy carbon electrode (AuNPs@TA-GCE). To the best of our knowledge, no strategy for the determination of Al^{3+} in combination with TA by voltammetry has been suggested in the past.

The presented work demonstrates a sensitive, reliable and cost-efficient alternative method for the detection of aluminium(III) in aqueous solutions. All voltammetric experiments were achieved using a freshly modified electrode. The reusability of the electrode was not assessed, as sensing principles are commonly transferred onto disposable screen printed electrodes in later steps.

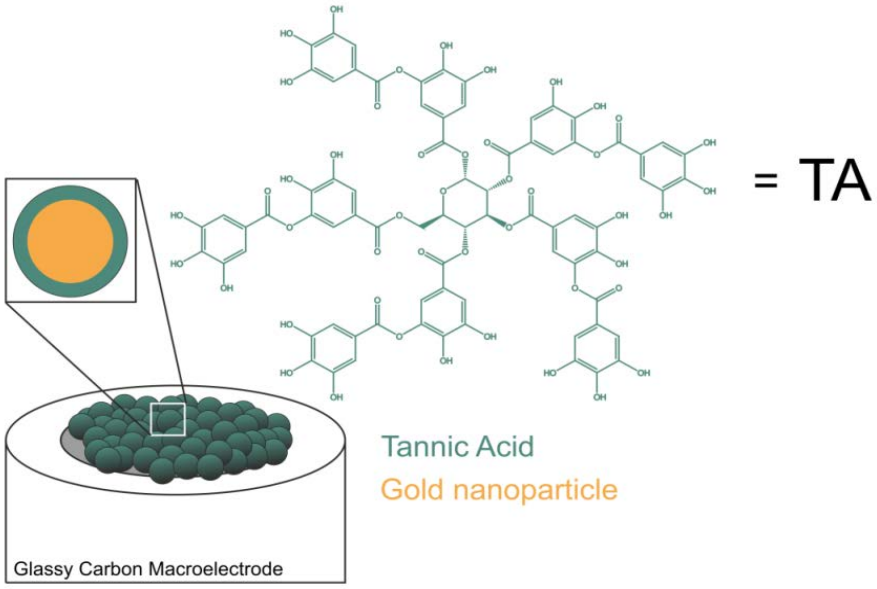

Scheme 1. Tannic acid and the AuNPs@TA-GCE.

2. Material and Methods

2.1. Chemicals

Tannic acid-capped gold nanoparticles (AuNPs@TA, 2.2 x 10^{10} particles mL^{-1}, NanoComposix, San Diego, USA), with a hydrodynamic diameter of 68 nm, as indicated by the manufacturer, were used as received. Tannic acid ($C_{76}H_{52}O_{46}$, average molecular mass 1701.2 $gmol^{-1}$, Sigma-Aldrich, Gillingham, UK) solutions were prepared freshly for all experiments since the compound can be oxidised and decomposed by exposure to light and atmospheric oxygen[30, 44]. Aluminium sulphate ($Al_2(SO_4)_3.16H_2O$, >97%, Alfa Aesar, Karlsruhe, Germany) was used as a source

of Al^{3+}. Where water is referred to, nanopure water with a resistivity not less than 18.2 MΩ cm at 25 ◦C (Millipore water purification system, Millipak Express 20, Watford, UK) was used. HCl-KCl solution solutions of pH1.0 and pH2.0 were prepared by mixing 97.0 mL of 0.1 M HCl and 3.0 mL of 0.1 M KCl (pH1.0) or by mixing 10.6 mL of 0.1 M HCl and 89.4 mL of 0.1 M KCl (pH2.0).[45]

2.2. Instrumental

All electrochemical measurements (cyclic voltammetry and square wave voltammetry) were carried out inside a Faraday cage at 25 ± 1 ◦C using a μ-Autolab Type III potentiostat (Metrohm u3AUT71335, Autolab B.V., Utrecht, The Netherlands) and data acquisition was controlled by GPES software (version 4.9). A three-electrode system was used for all electrochemical measurements. A 1.48 ± 0.02 mm radius glassy carbon electrode (GCE) and a 1 mm radius gold electrode were used as working electrodes (CH Instruments, USA). A saturated calomel electrode (SCE, Hg/Hg_2Cl_2, saturated KCl) functioned as a reference electrode and a platinum wire was used as a counter electrode.

The GCE and gold electrode was polished using microcloth polishing pads and a water-alumina mix (1.0, 0.3, 0.05 μm, 5 minutes on each grade, Buehler, IL, UK), rinsed with nanopure water, and dried under N_2 flow. All analyte solutions were degassed using a high purity N_2 flow (BOC Gases plc, UK) for 5 min before measurement. After polishing, the GCE was modified immediately by drop casting 25.8 μL of AuNPs@TA, which approximately corresponds to a surface concentration of one monolayer if the particles are uniformly dispersed on the surface. After drying under N_2 flow, the modified electrode (AuNPs@TA-GCE) was immediately used for electrochemical experiments. A gold electrode was used without further surface modification.

2.3. Characterisation

Size and aggregation/agglomeration state of the AuNPs@TA were characterized using Scanning Electron Microscopy (SEM, JSM-6500F, JEOL Ltd., Japan), with an accelerating voltage of 5 kV using a secondary electron imaging mode. A glassy carbon plate (MFCD00133992 GC plate, 3 mm thick, type 2, Lancashire, UK), cleaned in aqua regia, was used as an electron imaging substrate. After polishing, SEM samples were prepared by drop casting AuNPs@TA onto the GC plate surface. Microscopy images were analysed for particle size and distribution using ImageJ (National Institute of Health, USA) and OriginPro 2017.

3. Results and Discussion

In this section, we first present the electrochemical characterisation of solution phase TA and of immobilised AuNPs@TA. Subsequently, the complexation of Al^{3+} and the AuNPs@TA-GCE system is discussed by analysing the resulting peak currents during cyclic voltammetry and evaluating the effects of scan rate, the concentration of target analyte and the electrode exposure time to sample solutions. Finally, an evaluation of the experimental parameters for square wave voltammetry (SWV) is presented, optimizing the electroanalytical performance of the chemical sensor. We demonstrate that useful measurable detection for Al^{3+} is achieved below the reported practicable level for aluminium(III) in drinking water.

3.1. Solution Phase Electrochemistry of Tannic Acid

Solution phase TA was electrochemically characterised in aqueous acid by cyclic voltammetry using a 2.0 mm gold macroelectrode at varying pH, TA concentrations, scan rates, and electrode exposure times (**Figure 1**). After polishing, the macroelectrode was exposed to TA concentrations, ranging from 1.0 mM to 15.0 mM. Cyclic voltammetry measurements revealed an oxidation peak of TA at a peak potential of 0.58 V *vs* SCE at pH1.0 (**Figure 1a**) and a peak potential of 0.54 V *vs* SCE at pH2.0. The shift in peak potential with pH is consistent with the need for deprotonation prior to electron transfer and the difference of *ca* 40 mV suggests the loss of fewer protons than electrons. For a particular concentration of TA, the current was approximately independent of pH, consistent with the TA being fully protonated at the pHs studied and with literature reports[31, 46] of the pK_a of TA (range from 2.5 to 8.5), which were independently verified in our work which suggested the effective pK_a of TA is *ca* 3.7.

A linear peak current behaviour on scan rate was observed (**Figure 1b**), suggesting the TA oxidation on the macroelectrode surface is a surface-controlled (adsorption) process. Furthermore, the immersion time of the macroelectrode in a 1.0 mM TA solution, prior to CV analysis, was found to play an important role to maximise the oxidation of TA, as the prolonged exposure of the macroelectrode to TA results in the increased adsorption of TA to the electrode surface. By varying the exposure time from zero to 30 minutes at open circuit potential, a maximum peak current at 10 min was identified. The adsorption of TA onto macroelectrode surface and its electrochemical reaction is represented in equation (1), where *x* and *y* are discussed below.

$$TA_{(aq)} \rightleftharpoons TA_{(ads)} \xrightarrow{-xH^+,\ -ye^-} Products \qquad (1)$$

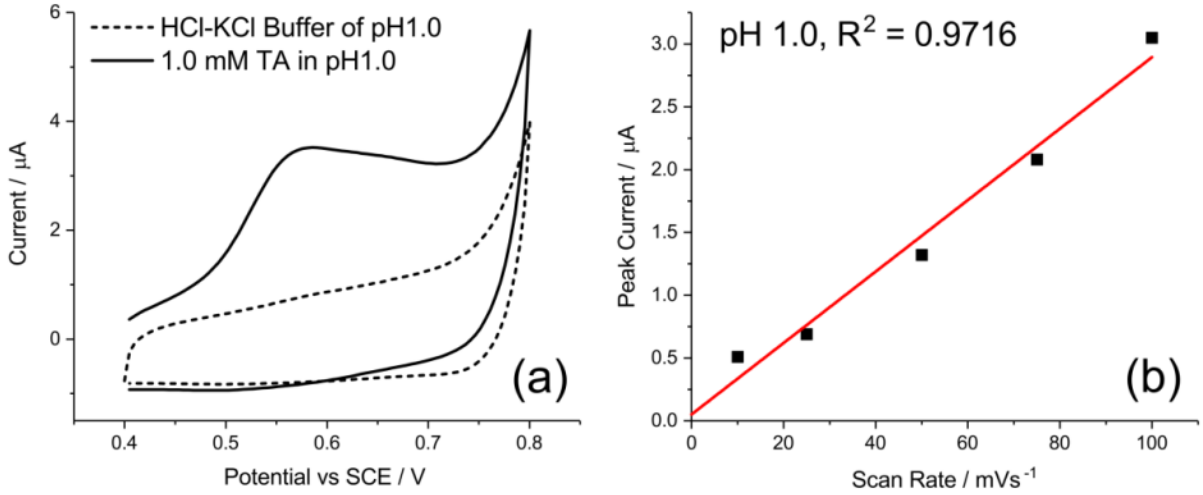

Figure 1. Electrochemical characterization of solution phase TA by cyclic voltammetry. (a) Cyclic voltammogram of 1.0 mM TA in HCl-KCl solution at pH1.0. (b) Linear peak current behaviour at various scan rates.

Next, the understanding of the electrochemical behaviour of TA in its combination with gold nanoparticles (AuNPs) is addressed in the following section.

3.2. Characterisation of AuNPs@TA

The size characterisation of the gold nanoparticles capped with tannic acid (AuNPs@TA) was carried out using scanning electron microscopy (SEM) using secondary electron imaging (SEI) mode. **Figure 2a** presents an SEM micrograph of AuNPs@TA, where a mean diameter size distribution of 60 ± 3 nm (standard deviation) was obtained (**Figure 2a, inset)**. The particle surface charge was quantified by measuring the zeta potential in nanopure water at 25 °C, whereby an average zeta potential of the AuNPs@TA of -30.9 ± 13.1 mV with a conductivity of 0.023 mS cm^{-1} was obtained. This value suggests a high stability of the colloidal gold dispersion.[47]

In agreement with literature[44, 46], an estimated effective radius of the TA molecules of 1.3 nm was calculated from the structure and known bond lengths and angles, corresponding to an area of *ca* 7 x 10^{-18} m^2 of nanoparticle surface, occupied per TA (**see S1 for calculation details**). Therefore, the amount of TA in one monolayer was estimated to be *ca* 1,750 molecules per nanoparticle.

Next, AuNPs@TA were electrochemically characterized by cyclic voltammetry in HCl-KCl solution at pH1.0, revealing an oxidation peak at a potential of 0.31 V *vs* SCE (**Figure 3a, blue curve**), attributed to the oxidation of TA[48] as illustrated in equation 1. For this purpose, a GCE was modified by drop casting *ca* 5.7 x 10^8 AuNPs@TA, corresponding to a surface concentration of nanoparticles of approximately one monolayer. This volume contains *ca* 10^{12} TA molecules in total (**see S1 for calculation details**).

Cyclic voltammetry of AuNPs@TA-GCE in HCl-KCl solution at pH1.0 at a range of scan rates between 25 and 100 mV s^{-1} showed a linear behaviour of the AuNPs@TA peak current as a function of scan rate (**Figure 2b**) suggesting that the oxidation process of AuNPs@TA at the GCE surface is a surface-controlled (adsorption) process. Furthermore, an investigation of the electrochemical current behaviour in dependence of the pH reveals a decrease in peak potential with increasing pH values (**Figure 2c**), along with a decrease in the peak currents. The response reflects the loss of protons on oxidation but the complexity of the TA structure precludes the quantification of the exact number of electrons and protons being transferred, except the sub-Nernstian slope of **Figure 2c** suggests $y >> x$.

Further, the effect of exposure time of the AuNPs@TA-GCE to the control solution, HCl-KCl solution at pH1.0, prior to voltammetric measurements were studied at zero and 30 min. The resulting peak at the potential of 0.31 V *vs* SCE exhibits a higher charge at 30 min compared to zero exposure time, suggesting the swelling of the capping agent layer on the AuNPs over prolonged exposure times. The exposure time prior to the CV being recorded plays a very important role to enable sensitivity of sensing performance, since it allows to improve the accessibility of the capping layers and to increase the possibility of Al^{3+} being complexed. However, the length of exposure time needs to meet reasonable time scale of analysis without compromising the sensitivity and linear range of the response. This is discussed further below.

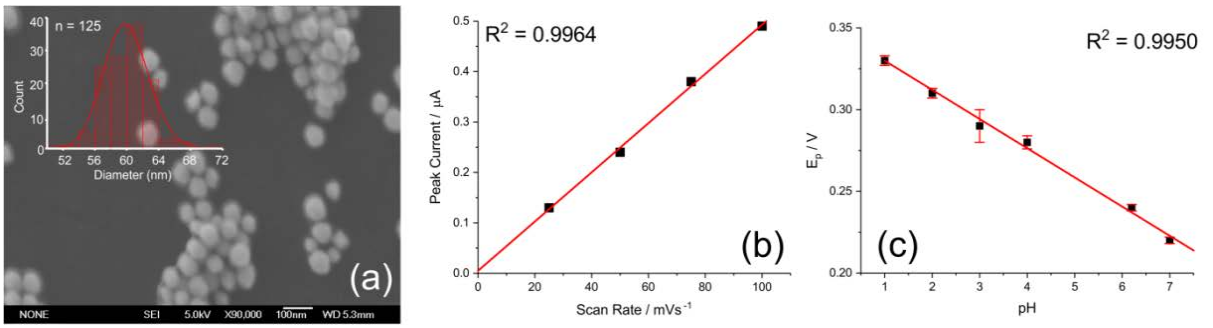

Figure 2. Characterisation of AuNPs@TA. (a) SEM micrograph of AuNPs@TA (inset: size distribution of AuNPs@TA). (b) The linear relationship between peak current and scan rate. (c) Dependence of peak potential on pH.

3.3. Complexation of Al^{3+} by AuNPs@TA

To explore the complexation of Al^{3+} by AuNPs@TA, cyclic voltammetry was performed in HCl-KCl solution at pH1.0, using first an unmodified glassy carbon electrode (GCE) in the presence of 2.0 mM Al^{3+} (**Figure 3a, red curve**). No Al^{3+} related signal was seen. After immobilization of AuNPs@TA at an approximate coverage of one monolayer of nanoparticles, the cyclic voltammogram exhibited an oxidation peak ("peak 1") at a potential of 0.31 V *vs* SCE (**Figure 3a, blue curve**), which, as above, is attributed to the oxidation of TA to form the TA-quinone (**Scheme 2, green**). By exposing the modified AuNPs@TA-GCE to 2.0 mM Al^{3+}, a second oxidation peak ("peak 2") becomes apparent at a potential of 0.52 V *vs* SCE (**Figure 3a, green curve**), which is attributed to the oxidation of TA complexed with Al^{3+} (**Scheme 2, red**). The possibility of a peak contribution from sulphate anions SO_4^{2-} of $Al_2(SO_4)_3$ (Al^{3+} source), was excluded after a control measurement in K_2SO_4 solution (**Figure 3a, black curve**). A peak charge of 0.14 μC, related to the number of TA oxidised per nanoparticle (**Figure 3a, green curve, peak-1**), and peak charge of 0.23 μC, related to the complexation of TA with Al^{3+} (**Figure 3a, green curve, peak-2**), were obtained by cyclic voltammetry at the scan rate of 100 mV s^{-1}.

Next, the effect of scan rate was addressed to identify whether the AuNPs@TA system in the presence of Al^{3+} is a surface-controlled or diffusion-controlled process. To assess this effect, a AuNPs@TA-GCE was immersed into a HCl-KCl solution at pH1.0 containing 2.0 mM Al^{3+} and cyclic voltammograms at a range of scan rates between 10 and 120 mV s^{-1} were obtained. **Figure 3b** presents the linear dependence of both peak currents on the scan rate, which suggests that the oxidation of Al^{3+}/AuNPs@TA complex is, as expected, a surface-controlled (adsorption) process, as with the oxidation of the uncomplexed TA. Note that "peak 1" is considerably enhanced in the presence of Al^{3+} suggesting that the partial complexation of the TA leads to a greater accessibility of the capping layers. The peak potentials for both peaks were essentially scan rate independent hinting at an electrochemically reversible process.

Furthermore, the electrochemical response with respect to Al^{3+} concentration during the complexation process was investigated by cyclic voltammetry. A AuNPs@TA-GCE was immersed in HCl-KCl solution at pH1.0 containing Al^{3+} at the relatively high concentrations from 0.1 to 10.0 mM. The results indicate that "peak 2" current resulting from Al^{3+}/AuNPs@TA complex increased monotonically with Al^{3+} concentration (**Figure S1a**), within the concentration range studied.

In addition, various surface coverages of AuNPs@TA on the GCE surface were analysed to find the optimal condition for Al^{3+} uptake during voltammetric measurements. The GCE surface was modified by drop casting varying amounts of AuNPs@TA, corresponding to surface coverages in a range of 0.1 to 1.5 monolayers (**Figure S1b**). After drop casting, the AuNPs@TA-GCE was immersed in HCl-KCl solution at pH1.0 containing 2.0 mM Al^{3+}. Increasing the amount of AuNPs@TA resulted in an increase of both peak currents during cyclic voltammetry. However, considering the cost of AuNPs@TA and the time required to modify the electrode surface, one-monolayer coverage was selected for further experiments.

Finally, the time of exposure of the modified electrode to the analyte solution, prior to voltammetric measurements (hereafter referred to as the "exposure time"), plays an important role during the optimization of the sensitivity of the sensing performance. The exposure time that generates a significant peak current increase, related to the detection of Al^{3+} within a reasonable timescale (<30 min) during cyclic voltammetry, was evaluated by immersing the AuNPs@TA-GCE in HCl-KCl solution at pH1.0 containing 2.0 mM Al^{3+} at various exposure times (**Figure S1c**). The peak current of "peak 2" increased continuously; a 30 min of exposure time was selected as giving good sensitivity.

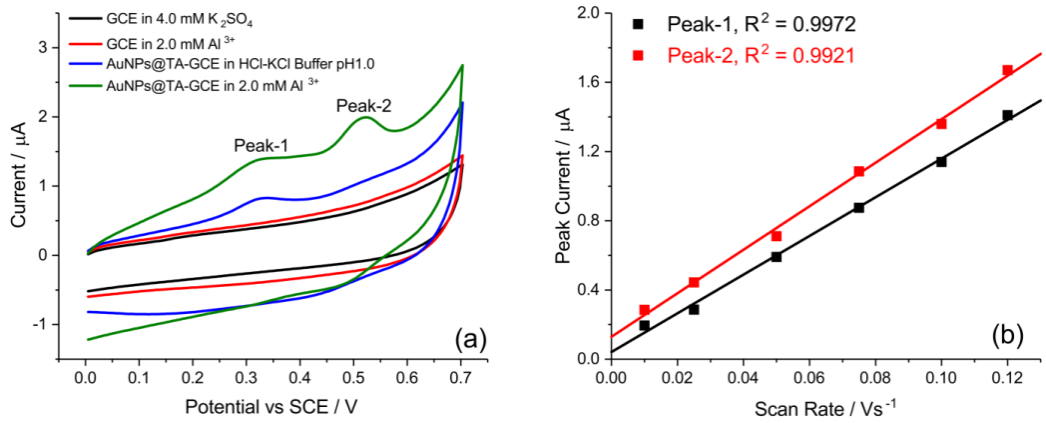

Figure 3. Characterization of Al^{3+} detection at GCEs. (a) Voltammograms of modified and unmodified GCE electrodes at a scan rate of 100 mV s^{-1}. (b) The linear relationship of peak currents at various scan rates.

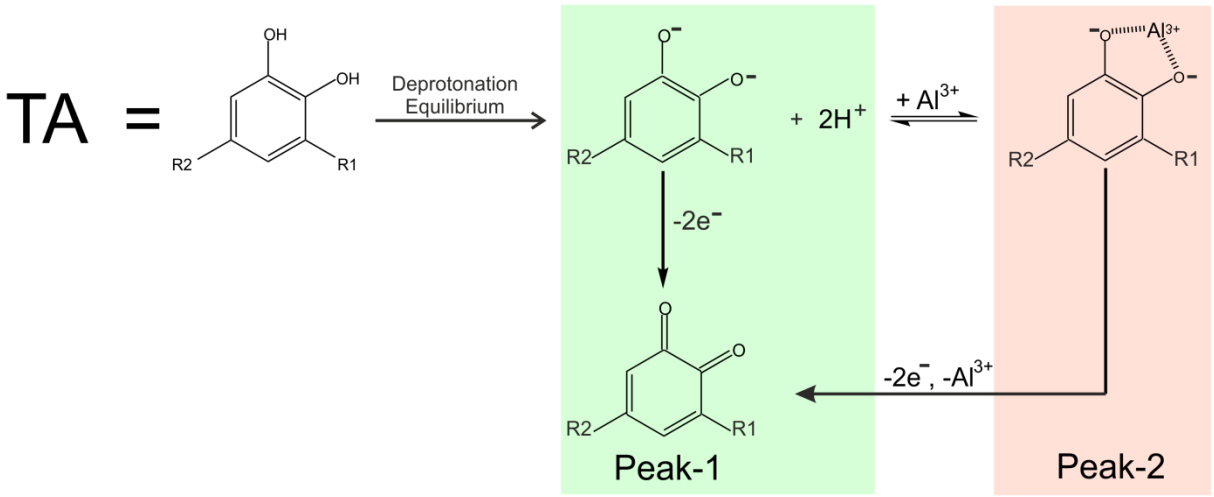

Scheme 2. TA exhibits several phenyl rings with acidic hydroxyl groups. These may be oxidized at *ca* 0.31 V *vs* SCE to yield peak-1 (**Figure 3a, green curve**). Solution Al^{3+} can be complexed by TA, raising its oxidation potential to that of "peak 2". Note the complexation of Al^{3+} may involve more than two deprotonated OH^- groups.

To assess the complexation process for analytical purposes, a AuNPs@TA-GCE was immersed into HCl-KCl solution at pH1.0, containing Al^{3+} at concentrations ranging from 10 pM to 10.0 mM with an exposure time of 30 min, and cyclic voltammograms at a scan rate of 100 mV s^{-1} were obtained. The amount species involved in the "peak 2" reaction, *n* (moles), was calculated from the peak charge, *Q* (Coulomb), obtained from cyclic voltammetry (**Figure S2a**) based on Faraday's law of electrolysis. To obtain the *effective* electrode coverage, Γ (mol cm^{-2}), the calculated number of moles was divided by the geometric area of the electrode, *A* (cm^2), as shown in equation (2),

$$\Gamma = \frac{Q}{zFA} \quad \textbf{(2)}$$

where *z* is the number of transferred electrons (*z*=2) and *F* is the Faraday constant (96485.33 C mol^{-1}).

To determine effective electrode coverage, a linear baseline correction was performed to measure the charge under the voltammetric peaks. As shown in **Figure 4**, a linear log-log relationship between the effective electrode coverage and the concentration of Al^{3+} in solution was observed for both "peak 1" and "peak 2", with an intercept of -10.79 $\pm$ 0.02 and -10.67 $\pm$ 0.02 respectively. In HCl-KCl solution at pH1.0 and 30 min exposure time, the presence of Al^{3+} resulted in significantly higher effective electrode coverage, compared to a control solution, lacking Al^{3+}. At a low concentrations of Al^{3+} (10.0 pM to 0.1 mM), the closely similar positive slope values of 0.097 $\pm$ 0.003 and 0.100 $\pm$ 0.002 for "peak 1" and "peak 2" respectively, indicate that the response of the TA capped is likely to reflect Al^{3+} induced swelling of the capping layer with an increased accessibility of chelating and oxidisable sites. The fact that the slope is below unity may indicate that the surface of the capping layer is partly saturated with Al^{3+}. Note, at higher concentrations of Al^{3+} (0.5 mM to 10.0 mM), "peak 2" increased strongly while "peak 1" remained relatively constant. For concentration above 0.1 mM, the effective electrode coverage of "peak 2" increased much more rapidly than "peak 1". Furthermore, standard deviations shown in **Figure 6**, result from experimental measurements in triplicates. These values remain relatively constant, indicating a good precision of the proposed methodology.

It should be noted that TA can form complexes with other ions. To address possible interferences from other ions, we carefully reviewed the literature reporting experimental stability constants of various ions and TA. The TA/Al^{3+} system is reported to have the highest stability constant of all metal/TA complexes. A table reporting the constants as well as experimental validation for Zn^{2+} ions can be found in the supporting information (**Table S1 and Figure S4**). Where no stability constants are recorded for ions, such as Cu(II), Ni(II) and Ca(II), available literature confirms no significant influence is expected due to insufficient binding of ions to TA at low pH or electrochemically inert complex formation.[30, 49, 50]

The effect of the exposure time of the AuNPs@TA-GCE to the analyte and a control solution was investigated. At zero exposure time (as represented by 1.0 µM and 0.1 mM Al^{3+}, **Figure 4**), the coverage of both "peak 1" and "peak 2" was lower compared to an exposure time of 30 min, suggesting the swelling degree of AuNPs@TA film, as noted above, was affected by lengthier exposure time and increased accessibility of the chelating sites.

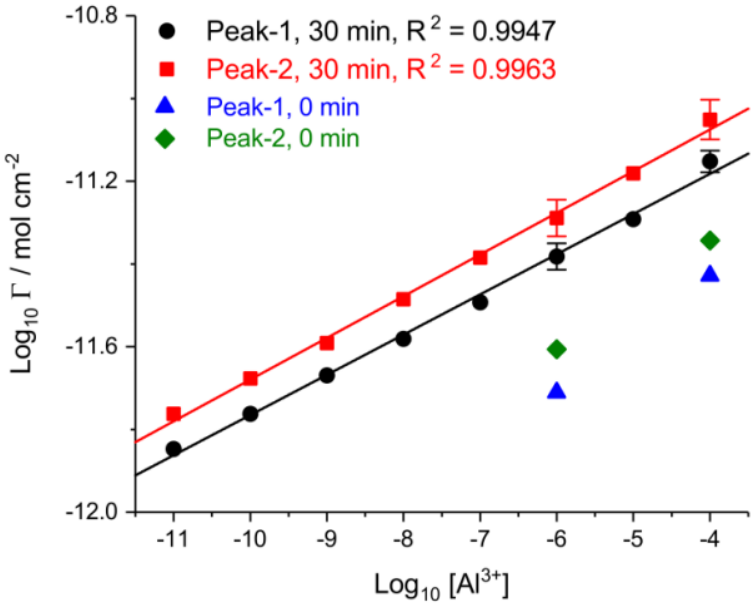

Figure 4. Dependence of the effective electrode coverage of the Al^{3+}/TA complex on the solution containing Al^{3+}. Note the log-log scale.

The above demonstrates a possible new analytical sensing method for Al^{3+}. However, the identified required exposure time of 30 minutes is disadvantageous for the routine monitoring and assessment of samples. In the following, we demonstrate that this aspect can be improved by conducting square wave voltammetry (SWV) analyses with the established sensing methodology.

3.4. Optimised Parameters of the Chemical Sensor

Given the high surface area of the modified electrode, capacitive and background currents can hide currents due to Al^{3+}/TA complex oxidation. By using square wave voltammetry (SWV), the capacitive current can be reduced. SWV in the present system requires careful optimisation of several analytical parameters, namely exposure potential and time, frequency, and pulse amplitude. To determine an optimum exposure time, a AuNPs@TA-GCE was immersed in HCl-KCl solution at pH1.0 containing 2.0 mM Al^{3+} and a holding potential of 0 V *vs* SCE was applied for exposure times ranging from 5 to 300 s. A potential sweep was carried out at a frequency of 40 Hz, and amplitude of 0.02 V. As shown in **Figure 5a**, "peak 2" was increased up to an exposure time of 300 s, after which a strong analytically useful signal is seen. This demonstrates a significant improvement in terms of time over the cyclic voltammetry approach and is reasonable for routine monitoring. The optimised parameters were independently validated at the lower concentration of 1.0 µM Al^{3+} (**Figure S5**).

Analysis of the operating frequency during SWV (**Figure 5b**) showed an increasing peak current for peak-2 up to 80 Hz, indicating optimal sensitivity for this parameter. Finally, the amplitude for SWV was examined. In the presence of 2.0 mM Al^{3+}, the pulse amplitude was varied from 0.01 to 0.1 V. As shown in **Figure 5c**, peak currents of peak-2 increased upon increase of the pulse amplitude up to 0.04 V, which was therefore selected as the optimum pulse amplitude for all subsequent experiments.

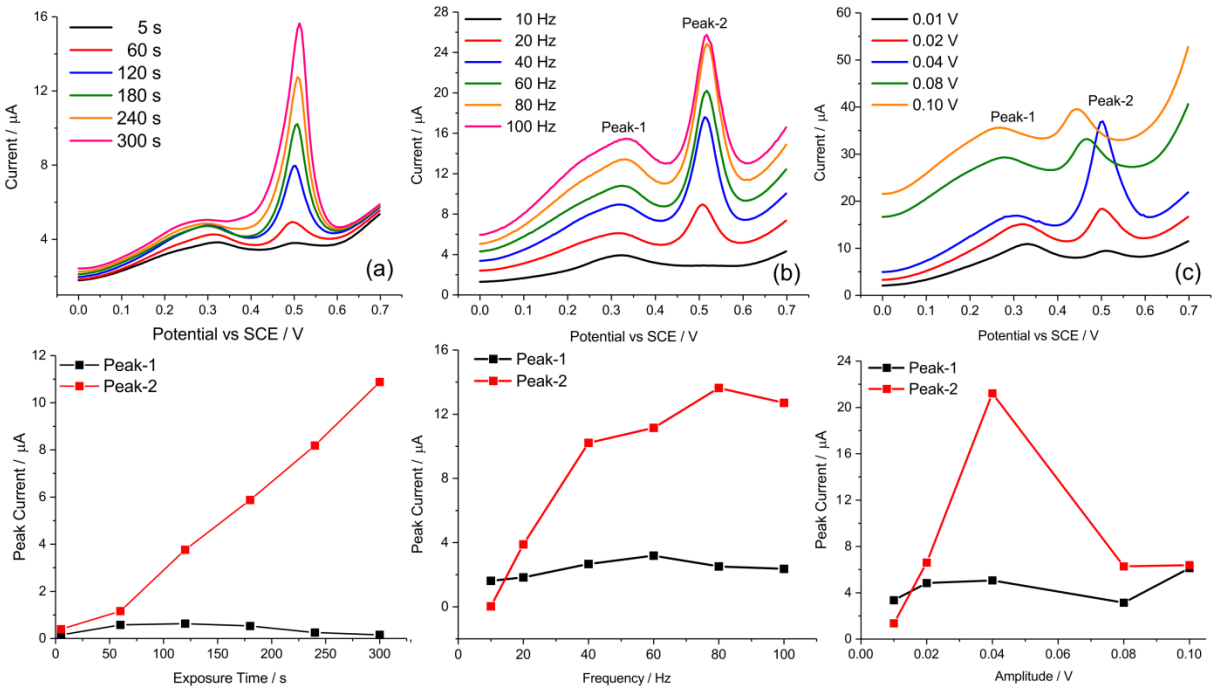

Figure 5. Parameter optimisation for SWV. Evaluating (a) exposure time, (b) frequency, and (c) amplitude for the AuNPs@TA-GCE system in HCl-KCl solution at pH1.0, containing 2.0 mM Al^{3+}.

3.5. Measurement of Low Concentrations of Al^{3+}

Having established a successful sensing strategy for the detection of Al^{3+} at AuNPs@TA-GCEs, the lower detectable levels were determined by SWV in HCl-KCl solution at pH1.0 by selecting a frequency of 80 Hz, a pulse amplitude of 0.04 V, and applying a holding potential of 0 V *vs* SCE for an exposure time of 300 s. **Figure 6a** shows that very clear signals are seen for concentrations of Al^{3+} in the range 0.1-10.0 µM corresponding to the range of interest for drinking water. Lower "measurable" signals were also extracted. The determined "measurable" lower limit here represents as the lowest concentration that can be distinguished significantly from the background signal. To determine a "measurable" lower limit for the proposed system, a polynomial (typically of order 3) fit was performed to extract the signal from the baseline. Subtracting the polynomial baseline from the original data, an electrochemical signal, significantly greater than the background (**Figure S3**), can be seen for concentrations as low as 10 pM (**Figure 6b)**. As shown in **Figure 6b**, a linear log-log relationship between the coverage (mol cm^{-2}) and the concentration of Al^{3+} in solution was observed for "peak 2" at concentrations ranging from 10.0 pM to 2.0 mM Al^{3+}. A linear trend was observed from 10.0 pM to 10.0 µM Al^{3+}. At concentrations exceeding 10.0 µM Al^{3+}, the modified electroactive area of the electrode probably tends to saturated with Al^{3+}. A "measurable" lower limit of 10.0 pM compares favourably with alternative methods[15, 20] while offering lower costs and the potential to be applicable in routine water quality assessments. A relative standard error of 39% for the determination of Al^{3+} concentration from the calibration curve was calculated (see supporting information for details). This error confirms the high sensitivity of the proposed method, as concentrations of even one order of magnitude below the critical limit of 7.4 µM, defined by the WHO, can be distinguished with statistical

significance. We note, however, that for use in heavily contaminated water, as opposed to drinking water, the possible effect of humic acid and/or surfactants might need to be investigated.

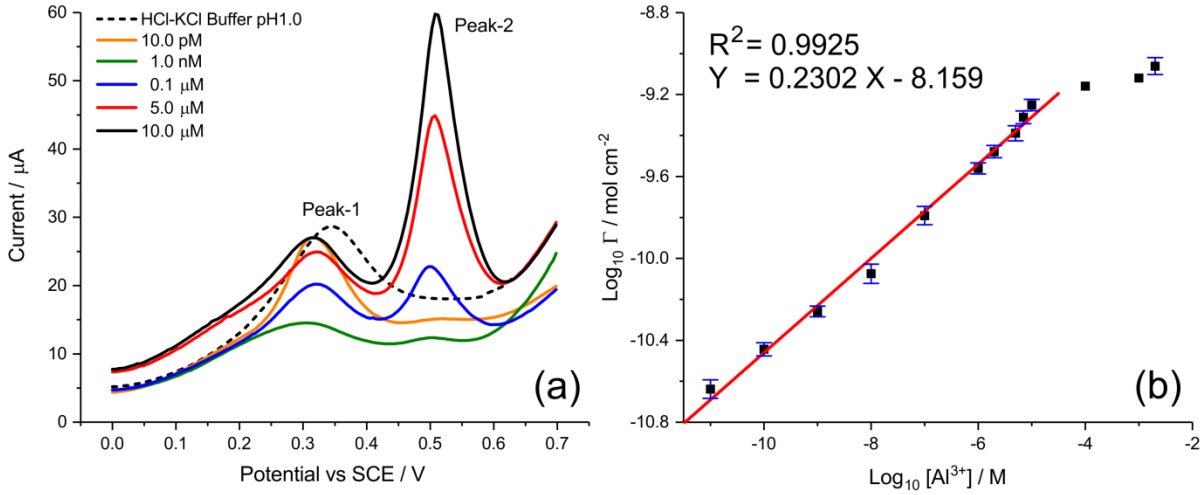

Figure 6. Determination of Al^{3+} by SWV. (a) Representative voltammograms of AuNPs@TA-GCE in the presence of Al^{3+}. (b) A linear log-log relationship between the effective electrode coverage and various Al^{3+} concentrations. Error bars represent the relative standard deviation.

4. Conclusions

An electrode modification method is presented, employing tannic acid-capped gold nanoparticles (AuNPs@TA) for the sensitive detection of Al^{3+} in water. SWV measurements revealed a "measurable" low limit of 10.0 pM and a linear range up to 10.0 μM, evidencing the excellent utility of the proposed analytical method.

Acknowledgements

A.L.S. thanks the Indonesia government through Indonesia Endowment Fund Scholarships (LPDP) for funding. S. K. thanks the support from the European Commission under the Marie Curie Programme (grant number 702009). The contents reflect only the authors' views and not the views of the European Commission.

Reference

[1] D. Krewski, R.A. Yokel, E. Nieboer, D. Borchelt, J. Cohen, J. Harry, S. Kacew, J. Lindsay, A.M. Mahfouz, V. Rondeau, Human health risk assessment for aluminium, aluminium oxide, and aluminium hydroxide, J. Toxicol. Environ. Heal. - Part B Crit. Rev. 10 (2007) 1–269. doi:10.1080/10937400701597766.

[2] Z. Wang, X. Wei, J. Yang, J. Suo, J. Chen, X. Liu, X. Zhao, Chronic exposure to aluminum and risk of Alzheimer's disease: A meta-analysis, Neurosci. Lett. 610 (2016) 200–206. doi:10.1016/j.neulet.2015.11.014.

[3] M. Chin-Chan, J. Navarro-Yepes, B. Quintanilla-Vega, Environmental pollutants as risk factors for neurodegenerative disorders: Alzheimer and Parkinson diseases, Front. Cell. Neurosci. 9 (2015). doi:10.3389/fncel.2015.00124.

[4] S.M. Ott, Renal Osteodystrophy—Time for Common Nomenclature, Curr. Osteoporos. Rep. 15 (2017) 187–193. doi:10.1007/s11914-017-0367-y.

[5] H.M.S. Wasana, G.D.R.K. Perera, P.S. De Gunawardena, J. Bandara, The impact of aluminum, fluoride, and aluminum–fluoride complexes in drinking water on chronic kidney disease, Environ. Sci. Pollut. Res. 22 (2015) 11001–11009. doi:10.1007/s11356-015-4324-y.

[6] World Health Organization, Guidelines for drinking-water quality, fourth edition, 2011.

http://www.who.int/water_sanitation_health/publications/2011/dwq_guidelines/en/%5Cnhttp://www.who.int/water_sanitation_health/publications/2011/dwq_chapters/en/#.VOAis9HLOE8.mendeley.
[7] E.J. Santos, E.B. Fantin, R.E. Paixão, A.B. Herrmann, R.E. Sturgeon, Spectrophotometric determination of aluminium in hemodialysis water, J. Braz. Chem. Soc. 26 (2015) 2384–2388. doi:10.5935/0103-5053.20150224.
[8] M. Frankowski, A. Zioła-Frankowska, I. Kurzyca, K. Novotný, T. Vaculovič, V. Kanický, M. Siepak, J. Siepak, Determination of aluminium in groundwater samples by GF-AAS, ICP-AES, ICP-MS and modelling of inorganic aluminium complexes, Environ. Monit. Assess. 182 (2011) 71–84. doi:10.1007/s10661-010-1859-8.
[9] S. Mazrura, M.R. Siti Farizwana, A. Zurahanim Fasha, G. Ahmad Rohi, Determination of aluminium and physicochemical parameters in the palm oil estates water supply at Johor, Malaysia, J. Environ. Public Health. 2010 (2010). doi:10.1155/2010/615176.
[10] B.B. Nanda, J.S. Brahmaji Rao, R. Kumar, R. Acharya, Determination of trace concentration of aluminium in raw rice samples using instrumental neutron activation analysis and particle induced gamma-ray emission methods, J. Radioanal. Nucl. Chem. 310 (2016) 1241–1245. doi:10.1007/s10967-016-5032-x.
[11] M.A. Qadir, M. Ahmed, S. Shahzad, Determination of Aluminium by Electrothermal Atomization Atomic Absorption Spectrometry in Serum to Characterize Hemodialysis Toxicity, Anal. Lett. 48 (2015) 147–153. doi:10.1080/00032719.2014.930872.
[12] M.A. Zanjanchi, H. Noei, M. Moghimi, Rapid determination of aluminum by UV–vis diffuse reflectance spectroscopy with application of suitable adsorbents, Talanta. 70 (2006) 933–939. doi:10.1016/j.talanta.2006.05.056.
[13] Y. Khanhuathon, W. Siriangkhawut, P. Chantiratikul, K. Grudpan, Spectrophotometric method for determination of aluminium content in water and beverage samples employing flow-batch sequential injection system, J. Food Compos. Anal. 41 (2015) 45–53. doi:10.1016/j.jfca.2015.02.002.
[14] S.D. Thomas, D.E. Davey, D.E. Mulcahy, C.W.K. Chow, Determination of aluminum by adsorptive cathodic stripping voltammetry with 1,2-Dihydroxyanthraquinone-3-Sulfonic Acid (DASA): Effect of thin mercury film electrode, Electroanalysis. 18 (2006) 2257–2262. doi:10.1002/elan.200503629.
[15] J. Zuziak, M. Jakubowska, Voltammetric determination of aluminum-Alizarin S complex by renewable silver amalgam electrode in river and waste waters, J. Electroanal. Chem. 794 (2017) 49–57. doi:10.1016/j.jelechem.2017.04.009.
[16] P. Deng, J. Fei, J. Zhang, Y. Feng, Determination of trace aluminum by anodic adsorptive stripping voltammetry using a multi-walled carbon nanotube modified carbon paste electrode, Anal. Lett. 44 (2011) 1521–1535. doi:10.1080/00032719.2010.520382.
[17] V. Arancibia, C. Muñoz, Determination of aluminium in water samples by adsorptive cathodic stripping voltammetry in the presence of pyrogallol red and a quaternary ammonium salt, Talanta. 73 (2007) 546–552. doi:10.1016/j.talanta.2007.04.009.
[18] L.B. Santos, M.T.F. de Souza, A.T. Paulino, E.E. Garcia, E.M. Nogami, J.C. Garcia, N.E. de Souza, Determination of aluminum in botanical samples by adsorptive cathodic stripping voltammetry as Al-8-hydroxyquinoline complex, Microchem. J. 112 (2014) 50–55. doi:10.1016/j.microc.2013.09.016.
[19] L. Qiong, W. Lirong, X. Danli, L. Guanghan, Determination of trace aluminum in foods by stripping voltammetry, Food Chem. 97 (2006) 176–180. doi:10.1016/j.foodchem.2005.05.003.
[20] S. Rana, S.K. Mittal, N. Singh, J. Singh, C.E. Banks, Schiff base modified screen printed electrode for selective determination of aluminium(III) at trace level, Sensors Actuators, B Chem. 239 (2017) 17–27. doi:10.1016/j.snb.2016.07.133.
[21] K. Wong, Q. Zeng, A. Yu, Gold catalysts: A new insight into the molecular adsorption and CO oxidation, Chem. Eng. J. 155 (2009) 824–828. doi:10.1016/j.cej.2009.09.006.
[22] S. Aswathy Aromal, D. Philip, Facile one-pot synthesis of gold nanoparticles using tannic acid and its application in catalysis, Phys. E Low-Dimensional Syst. Nanostructures. 44 (2012) 1692–1696. doi:10.1016/j.physe.2012.04.022.
[23] J.D.E.T. Wilton-Ely, The surface functionalisation of gold nanoparticles with metal complexes, Dalt. Trans. (2008) 25–29. doi:10.1039/B714144K.
[24] C. Pezzato, S. Maiti, J.L.-Y. Chen, A. Cazzolaro, C. Gobbo, L.J. Prins, Monolayer protected gold nanoparticles with metal-ion binding sites: functional systems for chemosensing applications, Chem. Commun. 51 (2015) 9922–9931. doi:10.1039/C5CC00814J.
[25] S.J. Cloake, H.S. Toh, P.T. Lee, C. Salter, C. Johnston, R.G. Compton, Anodic stripping voltammetry of silver nanoparticles: Aggregation leads to incomplete stripping, ChemistryOpen. 4 (2015) 22–26. doi:10.1002/open.201402050.
[26] K. Ngamchuea, K. Tschulik, S. Eloul, R.G. Compton, In Situ Detection of Particle Aggregation on Electrode Surfaces, ChemPhysChem. 16 (2015) 2338–2347. doi:10.1002/cphc.201500168.
[27] S. V. Sokolov, K. Tschulik, C. Batchelor-McAuley, K. Jurkschat, R.G. Compton, Reversible or Not? Distinguishing Agglomeration and Aggregation at the Nanoscale, Anal. Chem. 87 (2015) 10033–10039. doi:10.1021/acs.analchem.5b02639.
[28] E.A. Untener, K.K. Comfort, E.I. Maurer, C.M. Grabinski, D.A. Comfort, S.M. Hussain, Tannic acid coated gold nanorods demonstrate a distinctive form of endosomal uptake and unique distribution within cells, ACS Appl. Mater. Interfaces. 5 (2013) 8366–8373. doi:10.1021/am402848q.
[29] C.Y. Tsai, D.S. Lee, Y.H. Tsai, B. Chan, T.Y. Luh, P.J. Chen, P.H. Chen, Shrinking gold nanoparticles: Dramatic effect of a cryogenic process on tannic acid/sodium citrate-generated gold nanoparticles, Mater.

Lett. 58 (2004) 2023–2026. doi:10.1016/j.matlet.2003.12.019.
[30] B.H. Cruz, J.M. Díaz-Cruz, C. Ariño, M. Esteban, Heavy Metal Binding by Tannic Acid: A Voltammetric Study, Electroanalysis. 12 (2000) 1130–1137. doi:10.1002/1521-4109(200010)12:14<1130::AID-ELAN1130>3.0.CO;2-7.
[31] M.A. Rahim, H. Ejima, K.L. Cho, K. Kempe, M. Müllner, J.P. Best, F. Caruso, Coordination-driven multistep assembly of metal-polyphenol films and capsules, Chem. Mater. 26 (2014) 1645–1653. doi:10.1021/cm403903m.
[32] L. Fan, Y. Ma, Y. Su, R. Zhang, Y. Liu, Q. Zhang, Z. Jiang, Green coating by coordination of tannic acid and iron ions for antioxidant nanofiltration membranes, RSC Adv. 5 (2015) 107777–107784. doi:10.1039/C5RA23490E.
[33] A. Üçer, A. Uyanik, Ş.F. Aygün, Adsorption of Cu(II), Cd(II), Zn(II), Mn(II) and Fe(III) ions by tannic acid immobilised activated carbon, Sep. Purif. Technol. 47 (2006) 113–118. doi:10.1016/j.seppur.2005.06.012.
[34] L.C. Andriana Surleva, Petya Atanasova, Tinka Kolusheva, Study of the complex equilibrium between titanium (IV) and tannic acid, J. Chem. Technol. Metall. 49 (2014) 594–600. dl.uctm.edu/journal/node/j2014-6/10-Surleva_594-600.pdf.
[35] H. Luo, S. Zhang, X. Li, X. Liu, Q. Xu, J. Liu, Z. Wang, Tannic acid modified Fe3O4 core???shell nanoparticles for adsorption of Pb2+ and Hg2+, J. Taiwan Inst. Chem. Eng. 72 (2017) 163–170. doi:10.1016/j.jtice.2017.01.026.
[36] M.A. Badawi, N.A. Negm, M.T.H. Abou Kana, H.H. Hefni, M.M. Abdel Moneem, Adsorption of aluminum and lead from wastewater by chitosan-tannic acid modified biopolymers: Isotherms, kinetics, thermodynamics and process mechanism, Int. J. Biol. Macromol. 99 (2017) 465–476. doi:10.1016/j.ijbiomac.2017.03.003.
[37] P. Kraal, B. Jansen, K.G.J. Nierop, J.M. Verstraten, Copper complexation by tannic acid in aqueous solution, Chemosphere. 65 (2006) 2193–2198. doi:10.1016/j.chemosphere.2006.05.058.
[38] P. Meethale Kunnambath, S. Thirumalaisamy, Characterization and utilization of tannin extract for the selective adsorption of Ni (II) ions from water, J. Chem. 2015 (2015). doi:10.1155/2015/498359.
[39] T.B. Kinraide, A.E. Hagermann, Interactive intoxicating and ameliorating effects of tannic acid, aluminum (Al3+), copper (Cu2+), and selenate (SeO42-) in wheat roots: A descriptive and mathematical assessment, Physiol. Plant. 139 (2010) 68–79. doi:10.1111/j.1399-3054.2010.01347.x.
[40] T. Kolusheva, M. Hristova, L. Costadinnova, Study of the complex formation reaction between Al(III) and tannic acid, J. Univ. Chem. Technol. Metall. 47 (2012) 570–573. http://dl.uctm.edu/journal/node/j2012-5/14-Kolusheva_570-573.pdf.
[41] L. Zhang, R. Liu, B.W. Gung, S. Tindall, J.M. Gonzalez, J.J. Halvorson, A.E. Hagerman, Polyphenol-Aluminum Complex Formation: Implications for Aluminum Tolerance in Plants, J. Agric. Food Chem. 64 (2016) 3025–3033. doi:10.1021/acs.jafc.6b00331.
[42] S. Kim, S. Philippot, S. Fontanay, R.E. Duval, E. Lamouroux, N. Canilho, A. Pasc, pH- and glutathione-responsive release of curcumin from mesoporous silica nanoparticles coated using tannic acid–Fe(<scp>iii</scp>) complex, RSC Adv. 5 (2015) 90550–90558. doi:10.1039/C5RA16004A.
[43] Ş. Sungur, A. Uzar, Investigation of complexes tannic acid and myricetin with Fe(III), Spectrochim. Acta - Part A Mol. Biomol. Spectrosc. 69 (2008) 225–229. doi:10.1016/j.saa.2007.03.038.
[44] C. Poncet-Legrand, B. Cabane, A.-B. Bautista-Ortín, S. Carrillo, H. Fulcrand, J. Pérez, A. Vernhet, Tannin oxidation: intra- versus intermolecular reactions., Biomacromolecules. 11 (2010) 2376–2386. doi:10.1021/bm100515e.
[45] C. Mohan, A guide for the preparation and use of buffers in biological systems, Calbiochem. (2003) 18–21.
[46] T. Shutava, M. Prouty, D. Kommireddy, Y. Lvov, pH responsive decomposable layer-by-layer nanofilms and capsules on the basis of tannic acid, Macromolecules. 38 (2005) 2850–2858. doi:10.1021/ma047629x.
[47] S. Bhattacharjee, DLS and zeta potential - What they are and what they are not?, J. Control. Release. 235 (2016) 337–351. doi:10.1016/j.jconrel.2016.06.017.
[48] D.L. Vu, B. Ertek, Y. Dılgın, L. Červenka, Voltammetric determination of tannic acid in beverages using pencil graphite electrode., Czech J. Food Sci. 33 (2015) 72–76.
[49] R. V Barbehenn, M.M. Martin, Formation of insoluble and colloidally dispersed tannic acid complexes in the midgut fluid of Manduca sexta (Lepidoptera: Sphingidae): An explanation for the failure of tannic acid to cross the peritrophic envelopes of lepidopteran larvae, Arch. Insect Biochem. Physiol. 39 (1998) 109–117. d.
[50] P. Meethale Kunnambath, S. Thirumalaisamy, Characterization and utilization of tannin extract for the selective adsorption of Ni (II) ions from water, J. Chem. 2015 (2015).